

The Vertical Component of Epineutral Diffusion and the Dianeutral Component of Horizontal Diffusion

TIMOTHY J. OSBORN

Climatic Research Unit, University of East Anglia, Norwich, United Kingdom

(Manuscript received 24 March 1997, in final form 21 July 1997)

ABSTRACT

Observations of the time-mean thermohaline state of the world oceans are used to identify temperature gradients (and implied diffusive heat fluxes) both horizontally and on density surfaces. Two types of density surface are used: neutral and isopycnal, with the latter giving significantly different (and poorer) results. Along-neutral-surface (epineutral) heat fluxes are estimated to have a vertical component that is upward and strong in the upper 1500 m of the extratropical oceans, and weakly downward elsewhere. Horizontal heat diffusion has a Dianeutral component with a similar pattern of strong and weak fluxes, although almost all fluxes are toward water of greater density.

1. Introduction

This study presents results from an investigation of the diffusive heat fluxes implied by the observed thermohaline structure of the world oceans. In particular, it focuses on the different fluxes implied by the neutral surface system, the potential density system, and the horizontal/vertical system.

The strength of oceanic motion, and hence turbulent mixing/stirring, is anisotropic. It is strongest in a lateral direction and weakest in a quasi-vertical direction. This turbulence causes diffusion of heat, salinity, and other tracers to occur in a similarly anisotropic fashion (canonical thermal diffusivity in a lateral direction is $\approx 10^3 \text{ m}^2 \text{ s}^{-1}$, while it is only $\approx 10^{-5}$ – $10^{-4} \text{ m}^2 \text{ s}^{-1}$ in the quasi-vertical direction).

Many modeling studies that have used ocean general circulation models (OGCMs) have applied (e.g., Cox 1984), and still apply (e.g., Cubasch et al. 1995), these (or similar) diffusivities in the horizontal and vertical directions. Iselin (1939), and many others since, have suggested that the diffusion tensor should instead be aligned so that the strongest diffusion occurs along surfaces of constant potential density (isopycnal surfaces). If that is the case, then two types of error can occur in OGCMs that misrepresent diffusion by applying it horizontally and vertically. First, vertical diffusive fluxes may be underestimated if they are generated only by weak vertical diffusion because the much stronger is-

opycnal diffusion (that may have a significant vertical component) is omitted (Redi 1982; England 1993). Second, strong horizontal mixing can lead to spurious diapycnal fluxes of heat and salt (and hence density) when it is applied in regions with sloping isopycnals (Veronis 1975; McDougall and Church 1986).

Redi (1982) demonstrated how the diffusion tensor can be rotated from the horizontal/vertical directions (Cartesian coordinates) to the isopycnal/diapycnal directions (isopycnic coordinates) in OGCMs. England (1993) noted a considerable improvement in the representation of Antarctic Intermediate Water (AAIW) by a global OGCM when these suggestions were implemented. Even when such a rotation is employed, numerical diffusion will still occur in the horizontal direction—and for some numerical schemes can be quite significant. This numerical diffusion is due to the solution of the tracer advection equations, the maximum allowable isopycnal slope, and the background diffusivity required for stability (Gough and Lin 1995). A more recent scheme (Gent et al. 1995) enables some of these terms to be greatly reduced, even to zero (Hirst and McDougall 1996). The only way to rotate all of these terms to the isopycnal direction, however, is to solve the model equations in pycnic coordinates (e.g., see Bleck et al. 1992; Oberhuber 1993).

Due to the nonlinear nature of the equation of state for seawater, the thermal expansion and saline contraction coefficients vary with pressure in such a way that some energy is required to move a water parcel along an isopycnal surface (McDougall 1987). It is possible to define and identify *neutral surfaces* that require no such work to be done on water parcels that move along them. McDougall (1987) advocates that the diffusion

Corresponding author address: Dr. Timothy J. Osborn, Climatic Research Unit, University of East Anglia, Norwich NR4 7TJ, United Kingdom.
E-mail: t.osborn@uea.ac.uk

tensor be aligned to these surfaces, which can be quite different to isopycnal surfaces. Often, the terms isopycnal and diapycnal are also used when considering neutral surfaces. Here, however, the terminology of You and McDougall (1990) is used to clarify the reported comparisons—namely, epineutral and dianeutral for fluxes along and across neutral surfaces, respectively.

If the fluxes that occur when neutral surfaces are used are significantly different to those obtained on isopycnals, then even models that use the isopycnal mixing parameterization of Redi (1982), or that discretize the model into pycnic coordinates (Bleck et al. 1992; Oberhuber 1993), may not be doing quite the correct thing. Note that both the implementation by Cox (1987) of Redi's scheme and a more recent parameterization of ocean mixing (Gent et al. 1995) use neutral surfaces.

The aim of the present study is to identify the main locations and quantify the magnitude of the vertical components of isopycnal and epineutral diffusion and the dianeutral component of horizontal diffusivity. Observations of the temperature and salinity of the world oceans can be used to locate the density surfaces and the thermal gradients along and across them. Using estimates of the diffusivities, the implied diffusive heat fluxes can be computed. Heat fluxes are used here, but salinity fluxes could equally well be used.

2. Observational dataset

The analysis makes use of the long-term mean observations of ocean salinity and in situ temperature supplied by Levitus (1982). No seasonal effects are considered here; only annual means are used. All calculations were performed on a $1^\circ \times 1^\circ$ grid, with 32 unequally spaced levels. The formula of Bryden (1973) and the international equation of state for seawater (UNESCO 1981) were used to compute potential temperatures and densities from the in situ observations.

Grid points for which the isopycnal or neutral surface slopes could not be computed (i.e., where the surface passing through a point of interest intersects with the ocean surface or bathymetry before it reaches an adjacent gridpoint column) were removed from the analysis. Also removed were any grid points with apparent static instabilities in their potential densities (referenced to the local pressure for the neutral surface calculations or to the sea surface pressure for the isopycnal case).

3. Locating neutral surfaces

Neutral surfaces are defined by McDougall (1987), and his definition would be required if we needed to trace the location of an actual surface throughout the ocean. All that is required here, in fact, is the slope of the neutral surfaces (and the local potential temperature gradient along them) that pass through each grid point. This can be obtained by simply using potential density referenced to the pressure at the point of interest—the

isopycnal surface thus identified is tangential to the neutral surface of interest (McDougall 1987) and thus has the same slope.

The following procedure was applied at each grid point in the dataset to locate the neutral surface that passes through it:

- 1) Extract the in situ density ρ and the pressure P at the point. This is the potential density (referenced to pressure P) of the surface that is to be located.
- 2) For each water column immediately to the north, south, east, or west compute the potential density at all depths, referenced to pressure P . Locate the depth at which density ρ occurs (using linear interpolation between observational levels) and denote these depths by $z(N)$, $z(S)$, $z(E)$, and $z(W)$.
- 3) Given meridional and zonal grid spacings of Δx and Δy , the north–south slope of the neutral surface is given by $[z(S) - z(N)]/(2\Delta x)$ and the east–west slope by $[z(W) - z(E)]/(2\Delta y)$.

The north–south slope (zonal mean given in Fig. 1a) shows considerable structure in the upper 2000 m. (Note that, in all results presented here, we are not interested in the uppermost part of the ocean where turbulence enables strong dianeutral transport. Indeed, in the fully mixed layer, the neutral surfaces will be vertical.) In the mid and high latitudes the neutral surfaces slope downward toward the equator, as expected from thermocline ventilation theory (Luyten et al. 1983). In lower latitudes, they slope upward toward the equator, due to the surface Ekman divergence. But there is also a small reversal in direction either side of $5^\circ N$. In the deeper ocean some slopes are quite steep but are of alternating sign—perhaps indicating some lack of precision in the calculation or in the original dataset. With weaker stratification and fewer observations, the slope calculations in the deep ocean will be much more susceptible to error. Less confidence should be placed in the results of this study below 2000 m and in some of the highest latitudes because of these possible errors.

In the east–west direction (zonal mean shown in Fig. 1b) there is also more coherent structure in the upper ocean than in the deeper ocean. Overall, the slopes are weaker than those in the meridional direction. Below the subtropical gyres, there are large regions in which the neutral surfaces slope upward toward the east, also in agreement with thermocline ventilation theory (Luyten et al. 1983). Poleward of 40° of latitude, with the exception of a narrow band in the ACC region, the upper ocean shows the reverse—a slope downward to the east. In the upper 150 m below the equator, surfaces slope upward toward the east, in agreement with observations of the equatorial mixed layer and thermocline. In the deeper ocean, it is still possible to identify a mean slope up to the west, despite the noise. This is clearer in the global mean, peaking in magnitude at 3500-m depth, and may be associated with the neutral surfaces that surround dense deep western boundary currents.

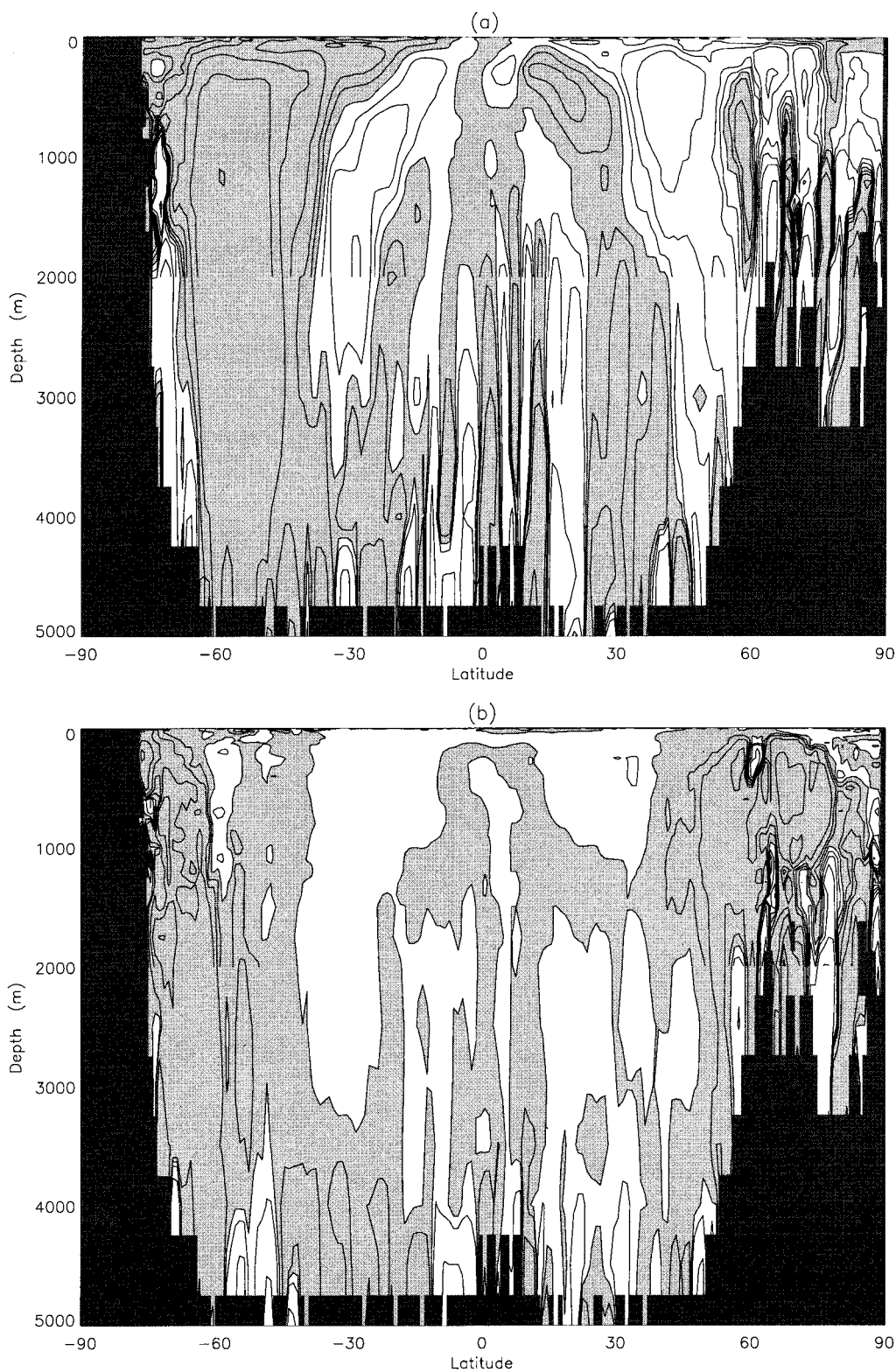


FIG. 1. Zonal mean of the slope of neutral surfaces in (a) a meridional direction and (b) a zonal direction; positive (unshaded) slopes indicate a slope upward to the north or east. Isolines have values of $(0, \pm 0.05, \pm 0.1, \pm 0.2, \pm 0.4, \pm 0.8, \pm 1.6, \pm 3.2, \text{ and } \pm 6.4) \times 10^{-3}$. Every second isoline is omitted below 2000 m.

The overall slope of the neutral surfaces increases with depth and latitude. The increase with depth may be due to the up–down–up–down alternating nature of the computed surfaces, with little net slope over long distances. Given that the deep ocean and the high latitudes are also the regions where the isotherms are likely to differ most from the neutral surfaces (since the effect of salinity on density is greatest at cold temperatures), it is likely that the vertical component of epineutral heat diffusion will be greatest in those regions too. Note, however, the earlier caveat regarding the accuracy of the results in some of these regions.

4. Vertical component of epineutral diffusion

a. Temperature gradients

The potential temperatures at depths $z(N)$, $z(S)$, $z(E)$, and $z(W)$ in the water columns to the north, south, east, and west of the current grid point were estimated by linear interpolation in the vertical and used to compute the along-neutral-surface potential temperature gradients. The sign of the gradients was adjusted so that a positive value indicates that temperature decreases as one moves down the surface, regardless of what geographical direction that is.

When zonally averaged, the epineutral temperature gradient in a meridional direction (Fig. 2a) shows that much of the ocean exhibits a cooling with depth (and hence freshening too) along neutral surfaces. The exception is the upper 2000 m of the mid and high latitudes, most of which show a warming (and hence salinification) with depth along neutral surfaces. This is also apparent in parts of the low latitudes, but only above 250 m of depth.

Despite the strongly alternating slope of the neutral surfaces in the deep ocean (Fig. 1a), the temperature gradient field is weaker and shows almost all one sign—that is, the temperature anomalies on the deep neutral surfaces covary with the slope of the surfaces in such a way that the combination of the fields cancels out the variations in sign. This suggests that the noise was not due to poor observational coverage or accuracy of temperature, but that either salinity is poorly observed or that there is a systematic lack of precision in the computation of the neutral surfaces in the deep ocean (e.g., the use of linear interpolation in finding potential density and temperature values).

The epineutral temperature gradient in a zonal direction shows a surprisingly similar pattern (Fig. 2b). Again, potential temperature decreases down neutral surfaces in the deep ocean and in much of the upper ocean between 40°S and 40°N. Above 1000 m and poleward of 40° of latitude, potential temperature increases down neutral surfaces. The pattern is weaker than that of the meridional component and is somewhat shallower.

This is evident in the globally averaged profiles of

the meridional and zonal components of the epineutral temperature gradients (not shown). In the former, there is a strong net warming with depth in the upper 600 m, and a weaker cooling with depth below this, while the zonal component shows a net warming with depth between 50 and 350 m in the global mean, and cooling elsewhere.

b. Diffusive fluxes

If the lateral thermal diffusivity is known, it can be multiplied by the along-neutral-surface temperature gradients (and the volumetric heat capacity of water) to find the epineutral heat flux. The thermal diffusivity at this grid scale is not well known since it must parameterize the effects of unresolved turbulent activity, but a commonly quoted value is $10^3 \text{ m}^2 \text{ s}^{-1}$ and that value is used here. Using a constant value such as this results in patterns of heat flux identical to the patterns of temperature gradients (the latter were shown in Fig. 2).

The epineutral heat fluxes in the zonal and meridional directions are then multiplied by the slope of the neutral surfaces to obtain the vertical component of the heat fluxes for both zonal and meridional gradients. These are then simply added together as scalars to obtain a field of the vertical component of the total along-neutral-surface diffusive heat flux.

At a very few grid points this vertical flux reaches 30 W m^{-2} , some upward and some downward. When zonally averaged (Fig. 3a) the maximum fluxes are almost 20 W m^{-2} (again, some upward, some downward) in parts of the high latitudes of both hemispheres. The fluxes are still in coherent patterns: there is a net *upward* flux of heat in the mid to high latitude upper ocean, and a net *downward* flux elsewhere ($<1 \text{ W m}^{-2}$ in the low-latitude ocean, greater in high latitudes at depth). The upward flux is particularly strong ($>10 \text{ W m}^{-2}$) in the region of the Antarctic Circumpolar Current and AAIW formation. This supports the work of England (1993), who found that including “isopycnal” (in fact epineutral) diffusion in an OGCM improves the characteristics and volume of the model’s AAIW. These results indicate that a similar improvement might be obtained in the Northern Hemisphere because epineutral diffusion is important in driving vertical fluxes there too (Fig. 3a). In fact, it is only in the Atlantic that these Northern Hemisphere fluxes extend below 500 m, implying that it is an active thermohaline circulation that yields the appropriate thermohaline structure to drive diffusive fluxes with a penetrating vertical component.

While heat fluxes have been the focus of this study, epineutral diffusion implies no flux of density. All heat fluxes are, therefore, accompanied by fluxes of salinity of the appropriate magnitude to result in zero density flux. The pattern of heat flux (Fig. 3a) provides a guide to the pattern of these salinity fluxes, but they will not be identical because salinity has a changing impact on

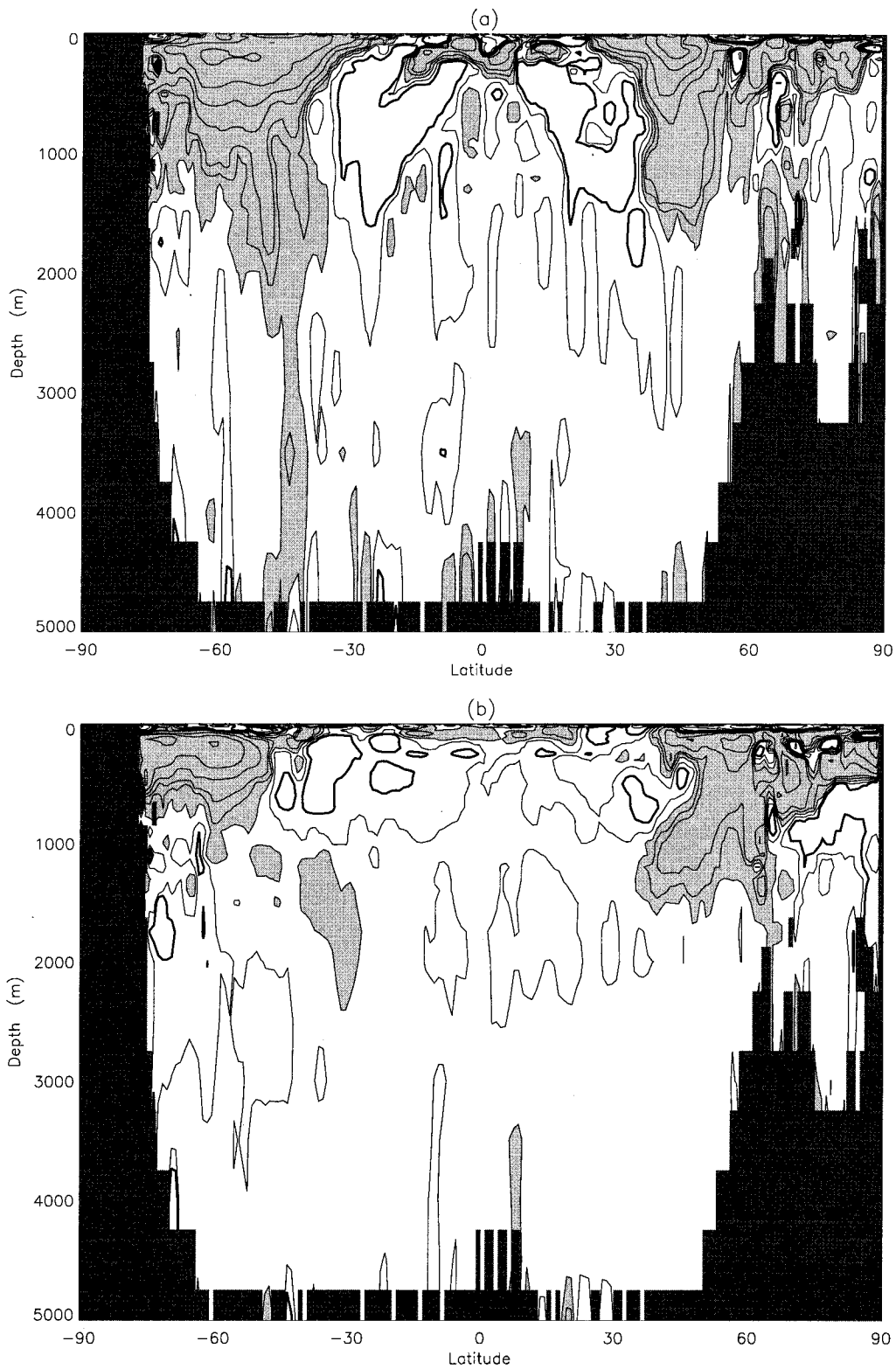


FIG. 2. Zonal mean of (a) the meridional component and (b) the zonal component of epineutral temperature gradient (K km^{-1}); positive (unshaded) gradients indicate a cooling with depth. Isolines have values of $(0, \pm 0.1, \pm 0.2, \pm 0.5, \pm 1, \pm 2, \pm 4, \text{ and } \pm 8) \times 10^{-3}$, with $+0.2 \times 10^{-3}$ thicker.

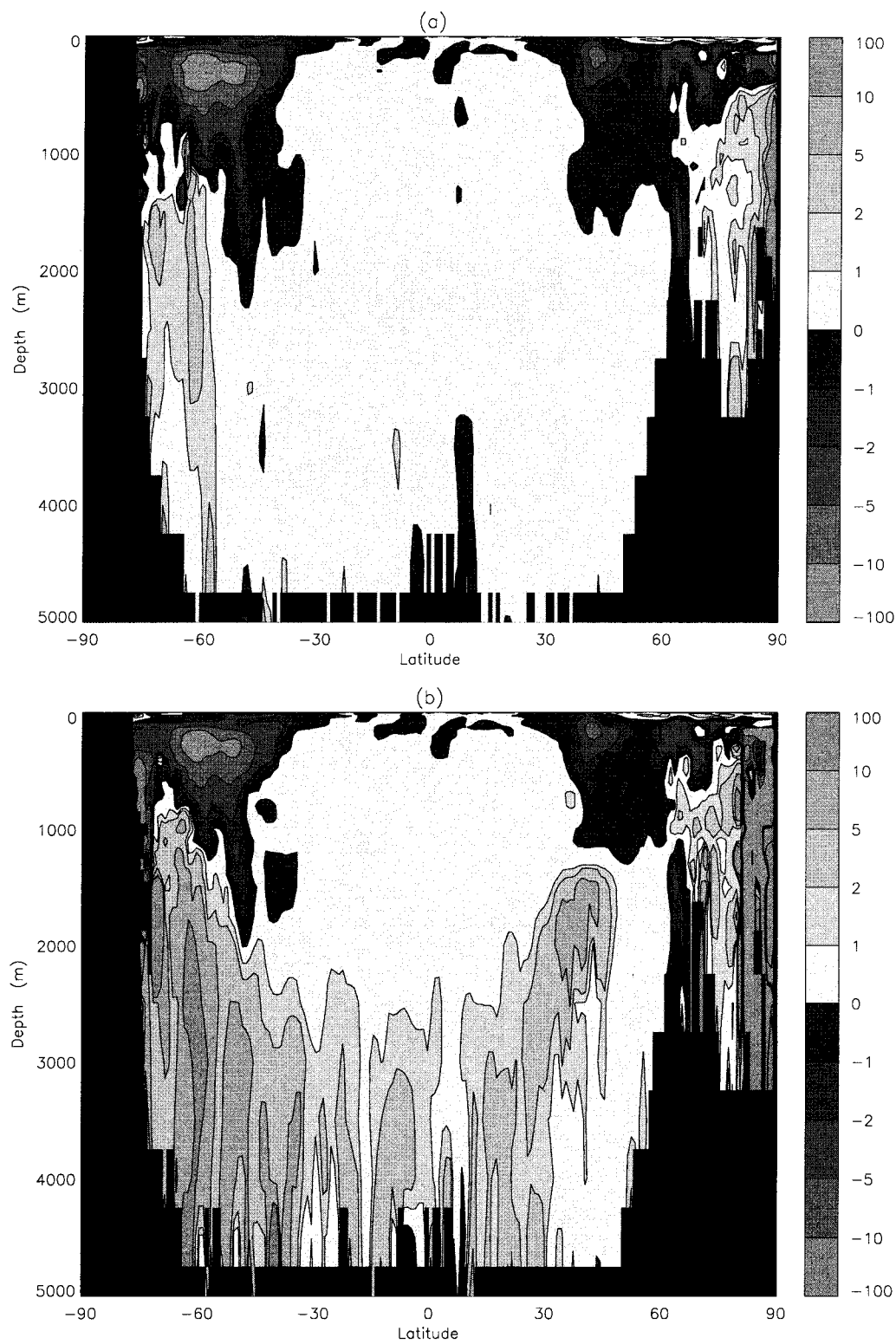


FIG. 3. Zonal mean of the vertical component of the estimated (a) along-neutral and (b) along-isopycnal surface diffusive heat flux (W m^{-2}). Positive values (paler shading) indicate a downward flux.

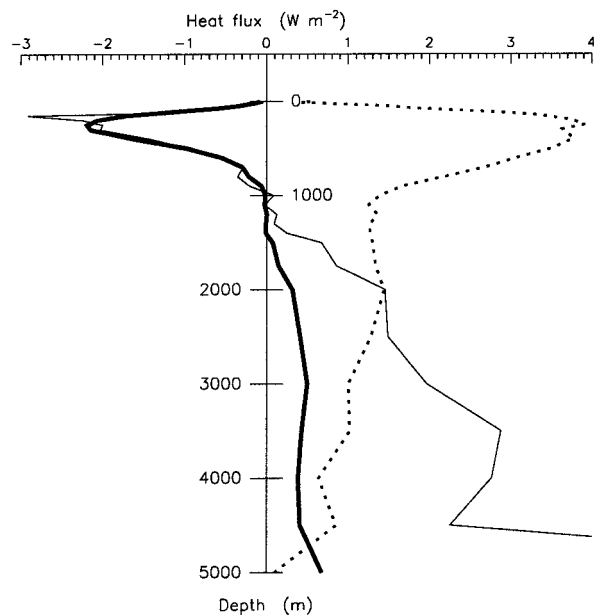


FIG. 4. The global-mean profiles (W m^{-2}) of the vertical component of the estimated epineutral (thick line) and isopycnal (thin line) diffusive heat fluxes and of the dianeutral component of the estimated horizontal heat fluxes (dotted line).

density through the nonlinear equation of state (UNESCO 1981).

In the global mean (Fig. 4), the high latitudes dominate the upper 1000 m, driving an upward heat flux that peaks at 2.2 W m^{-2} at 300 m. Below 1300 m, the net flux is downward, with a magnitude that remains below 0.8 W m^{-2} . The assumption (e.g., Hoffert and Flannery 1985) that the diffusive heat flux along density surfaces is insignificant in the vertical is proven to be false—the peak fluxes shown in Fig. 4 have the same order of magnitude as the net global-mean fluxes due to upwelling and diapycnal diffusion.

c. Isopycnal surfaces

It was noted earlier that some modeling and analytical studies specify mixing along isopycnal surfaces (i.e., of constant potential density referenced to sea surface pressure). This section addresses the issue of whether such an approach has a large effect on the heat fluxes under consideration here. Previous work (e.g., McDougall 1987) suggests this to be the case in some regions; the comparison is now extended to the global ocean. All calculations have, therefore, been repeated but by identifying the surfaces with constant potential density when referenced to the pressure at the sea surface.

In agreement with the findings of McDougall (1987) and You and McDougall (1990), neutral surfaces (Fig. 1) have weaker slopes than corresponding isopycnal surfaces (not shown) in many locations. The zonal mean patterns of both meridional and zonal slopes are very similar, but the isopycnals have stronger magnitudes and

noisier structure below 2000 m and in the high latitudes. Away from the high latitudes, only the Indian and North Atlantic Oceans show significant differences above 2000 m, with isopycnals being steeper than neutral surfaces overall.

The temperature gradients along the isopycnals (not shown) are quite different in the high latitudes and the deep ocean from those along neutral surfaces (Fig. 2). The gradient patterns are more extreme and show less coherent patterns in the Arctic Ocean, compared to those on neutral surfaces. Elsewhere, the cooling down isopycnal surfaces is much stronger than when neutral surfaces are used (unshaded areas in Fig. 2). Regions with gradients of more than $+0.2 \times 10^{-3} \text{ K km}^{-1}$ (thick isoline in Fig. 2) occur throughout the zonal means in both directions when isopycnals are used, frequently extending to the ocean bottom. The regions of warming down density surfaces in the mid- to high-latitude upper ocean (shaded areas in Fig. 2) extend less deeply when isopycnal surfaces are used.

The effect of these changes is that the vertical component of along-isopycnal heat diffusion shows a somewhat different pattern (Fig. 3b) than when neutral surfaces are used (Fig. 3a). The pattern is considerably less coherent in the Arctic Ocean when isopycnal surfaces are used. Strong fluxes in the deep ocean (Fig. 3b) appear to be an artifact of the use of isopycnal surfaces since they are much reduced on neutral surfaces (Fig. 3a).

These results are consistent with those of McDougall (1987), who also found that horizontal gradients of potential temperature tended to be overestimated on isopycnal surfaces compared to neutral surfaces. The increased noise is also clear in the global average of this vertical component of isopycnal diffusive heat flux (Fig. 4), as are the erroneously stronger fluxes in the deep ocean.

5. Dianeutral component of horizontal diffusion

The second term that is of interest is the dianeutral component of horizontal diffusive heat fluxes. It is this term that can lead to a spurious flux of heat (and hence density) across density surfaces, and it will occur in OGCMs that apply explicit diffusion in a horizontal direction and, to a lesser extent, in those that solve the tracer equations in a horizontal direction (thereby generating numerical diffusion). Such spurious fluxes can affect the dynamics of the ocean models (Veronis 1975; Gough and Lin 1995).

The horizontal potential temperature gradients were computed from the Levitus dataset both zonally and meridionally, and then adjusted in sign (by referring to the slope of the neutral surface passing through the current grid point, calculated in section 3) so that a positive value indicates that temperature decreases as one moves in the direction of increasing (locally referenced) potential density.

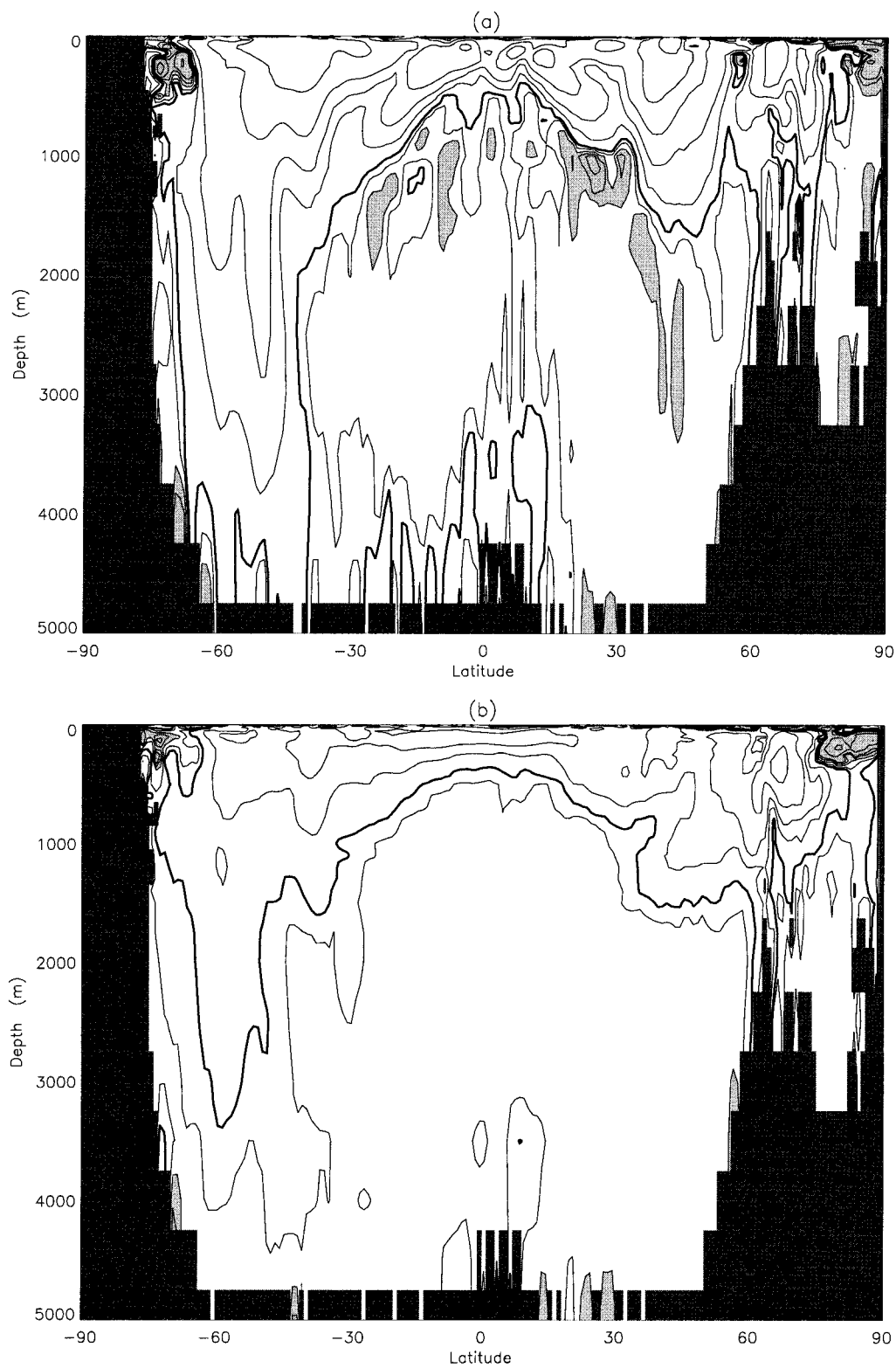


FIG. 5. Zonal mean of (a) the meridional component and (b) the zonal component of horizontal temperature gradients (K km^{-1}); gradients were first adjusted so that cooling with increased density is a positive gradient. Shading and isolines as in Fig. 2.

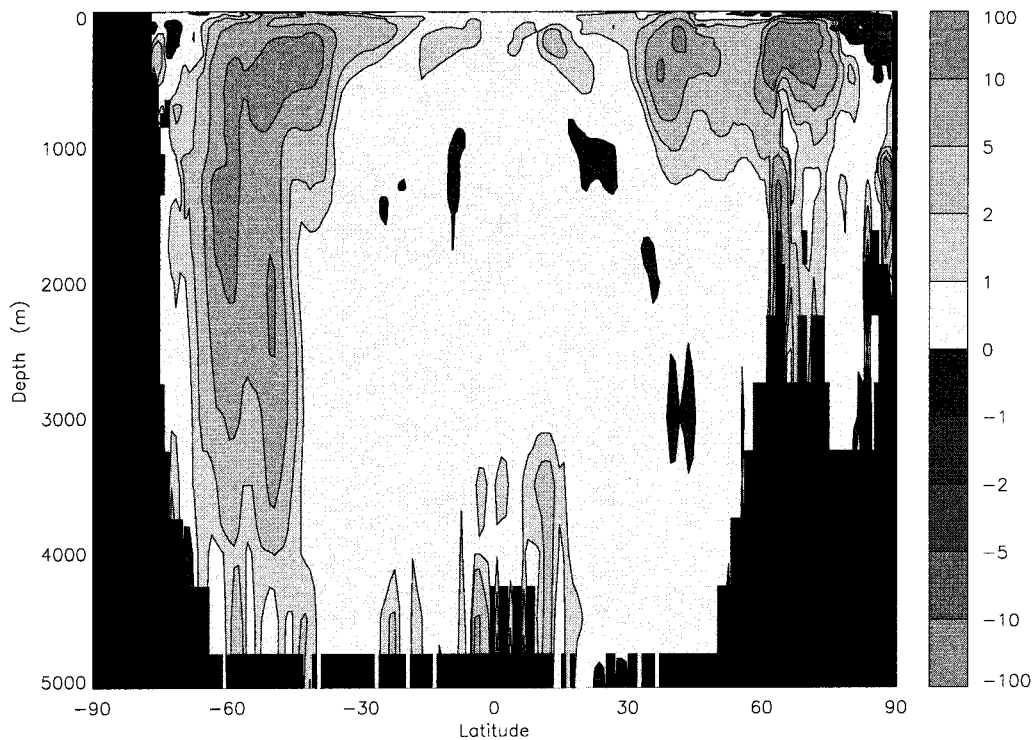


FIG. 6. Zonal mean of the diapycnal component of the estimated horizontal diffusive heat flux (W m^{-2}). Positive values (paler shading) indicate a flux into denser layers.

Again, only zonal mean results are shown (Fig. 5a for the meridional component and Fig. 5b for the zonal component). As with the epineutral temperature gradients (Fig. 2), these horizontal temperature gradients show a similar pattern in both directions, with the main differences again being that the east–west gradients are weaker and show a shallower pattern than the north–south gradients.

With temperature dominating the equation of state under most conditions, it is not surprising that there is usually a horizontal temperature decrease in the direction of increasing density. These gradients are strongest in the upper 500 m, with regions of somewhat weaker gradient extending more deeply in the mid (and some high) latitudes. Only in the highest latitudes (and below the low-latitude thermocline for the north–south component only) can one move horizontally in a direction of increasing density and find warmer temperatures (and, therefore, increased salinity).

If horizontal explicit and/or numerical diffusion is applied to these temperature gradients, heat fluxes will occur. As an example, a diffusivity of $10^3 \text{ m}^2 \text{ s}^{-1}$ is used again (but note that numerical diffusion would be considerably weaker than this). It is only when the neutral surfaces are inclined that these horizontal fluxes can cross them. To compute the diapycnal component of the horizontal fluxes, therefore, the heat fluxes are multiplied by the slope of the neutral surfaces that pass

through each point. The two directional components are evaluated separately and then summed.

Despite the upper-ocean temperature gradients being as large in the low latitudes as in the higher latitudes, the diapycnal component (Fig. 6) of the horizontal heat fluxes are weaker because the slope of the neutral surfaces is lower there. It is in the mid to high latitudes that horizontal diffusion will generate diapycnal heating of denser layers. These regions of heating extend to the ocean floor in the Southern Hemisphere, but only to about 1000 m in the Northern Hemisphere mean (to 800 m in the North Pacific and 1600 m in the North Atlantic). This diapycnal heating peaks at over 10 W m^{-2} in the zonal mean. In the global mean (Fig. 5), the peak is at almost 4 W m^{-2} in the upper 1000 m, and the fluxes are always in the direction of increased density (even though the zonal mean showed some limited regions with fluxes in the reverse direction).

6. Discussion and conclusions

The long-term annual mean climatology of Levitus (1982) has been analyzed to estimate some of the components of heat diffusion in the ocean. These components have been used to highlight the differences between the application of diffusion horizontally and vertically rather than along (epi-) and across (dia-) neutral surfaces. Some seasonally varying frontal regions will

be smoothed in the annual means used here; thus, some extreme values may have been reduced slightly in the present analysis. The coherent nature of the final results suggests that the Levitus (1982) dataset is sufficiently accurate to make these estimates, even in the deep ocean and the high latitudes. Some of the intermediate results were, however, rather noisy in these regions. The use of isopycnal surfaces (with potential density referenced to sea surface pressure) increased this noise and also gave dramatically different results in the deep ocean and in the Arctic Ocean.

It has been shown that isotherms and neutral surfaces differ sufficiently (due to salinity variations) to allow significant epineutral potential temperature gradients to exist. If arbitrary lateral diffusion is applied to these gradients, the implied heat fluxes can be estimated; due to the slope of the neutral surfaces, the vertical component of this epineutral diffusive heat flux is significant in certain regions. These regions are the upper 1500 m of the mid- to high-latitude oceans (shallower in oceans with weaker thermohaline activity) where there is a strong ($>10 \text{ W m}^{-2}$ in parts of the zonal mean) upward flux of heat. Elsewhere there is a coherent (but mostly much weaker) downward heat flux due to along-neutral-surface diffusion.

The slope of the neutral surfaces also means that applying horizontal diffusion to the temperature field will generate heat fluxes (and salinity and density fluxes) across density surfaces. These dianeutral fluxes are spurious and represent an unwanted flux of heat from less dense to more dense water layers—with consequent dynamical effects in an OGCM (Veronis 1975; Gough and Lin 1995). They are strongest in the mid- to high-latitude oceans (extending down to the ocean floor in the Southern Hemisphere and to 1200 m in the Northern Hemisphere)—that is, very similar regions to where the vertical component of the epineutral heat fluxes acted most strongly.

The main implications of the results presented here are for ocean general circulation models. They indicate the location and possible magnitude of the fluxes omitted when along-neutral-surface mixing is not modeled and they indicate the location and possible magnitude of the spurious diapycnal fluxes induced when horizontal mixing is modeled. That the fluxes are quite different when neutral surfaces (McDougall 1987) are used rather than isopycnal surfaces suggests that even models that discretize the ocean into pycnic coordinates (Bleck et al. 1992; Oberhuber 1993) may not be doing quite the correct thing.

The advantage of the present study over diagnosing these fluxes from an OGCM, is that those fluxes depend upon the simulated thermohaline structure, which may be somewhat different to (and therefore in error with) the observed ocean. These results could be used as a further validation of an OGCM to assess the simulated fluxes of heat (and salt) along neutral surfaces. The only

viable tools with which to investigate whether these fluxes might alter significantly with ocean state are, however, OGCMs.

Acknowledgments. This research was supported by the U.S. Dept. of Energy (DE-FG02-86ER60397). Discussions with Tom Wigley and the comments of two reviewers are gratefully acknowledged.

REFERENCES

- Bleck, R., C. Rooth, D. Hu, and L. T. Smith, 1992: Salinity-driven thermocline transients in a wind- and thermohaline-forced isopycnal coordinate model of the North Atlantic. *J. Phys. Oceanogr.*, **22**, 1486–1505.
- Bryden, H., 1973: New polynomials for thermal expansion, adiabatic temperature gradient and potential temperature of sea-water. *Deep-Sea Res.*, **20**, 401–408.
- Cox, M. D., 1984: A primitive equation 3-dimensional model of the ocean. GFDL Ocean Group Tech. Rep. 1, 143 pp. [Available from GFDL, P.O. Box 308, Princeton, NJ 08542.]
- , 1987: Isopycnal diffusion in a Z-coordinate ocean model. *Ocean Modelling* (unpublished manuscripts), **74**, 1–5.
- Cubasch, U., G. Hegerl, A. Hellbach, H. Hock, U. Mikolajewicz, B. D. Santer, and R. Voss, 1995: A climate simulation starting in 1935. *Climate Dyn.*, **11**, 71–84.
- England, M. H., 1993: Representing the global-scale water masses in ocean general circulation models. *J. Phys. Oceanogr.*, **23**, 1523–1552.
- Gent, P. R., J. Willebrand, T. J. McDougall, and J. C. McWilliams, 1995: Parameterizing eddy-induced tracer transports in ocean circulation models. *J. Phys. Oceanogr.*, **25**, 463–474.
- Gough, W. A., and C. A. Lin, 1995: Isopycnal mixing and the Veronis effect in an ocean general circulation model. *J. Mar. Res.*, **53**, 189–199.
- Hirst, A. C., and T. J. McDougall, 1996: Deep-water properties and surface buoyancy flux as simulated by a z-coordinate model including eddy-induced advection. *J. Phys. Oceanogr.*, **26**, 1320–1343.
- Hoffert, M. I., and B. P. Flannery, 1985: Model projections of the time-dependent response to increasing carbon dioxide. *Projecting the Climatic Effects of Increasing Carbon Dioxide*, M. C. MacCracken and F. M. Luther, Eds., U.S. Dept. of Energy, 149–190.
- Iselin, C. O'D., 1939: The influence of vertical and lateral turbulence on the characteristics of the waters at mid-depths. *EOS Trans. Amer. Geophys. Union*, **20**, 414–417.
- Levitus, S., 1982: *Climatological Atlas of the World Ocean*. NOAA Prof. Paper No. 13, U.S. Dept. of Commerce, Washington, DC, 173 pp.
- Luyten, J., J. Pedlosky, and H. Stommel, 1983: The ventilated thermocline. *J. Phys. Oceanogr.*, **13**, 292–309.
- McDougall, T. J., 1987: Neutral surfaces. *J. Phys. Oceanogr.*, **17**, 1950–1964.
- , and J. A. Church, 1986: Pitfalls with the numerical representation of isopycnal and diapycnal mixing. *J. Phys. Oceanogr.*, **16**, 196–199.
- Oberhuber, J. M., 1993: Simulation of the Atlantic circulation with a coupled sea ice–mixed layer–isopycnal general circulation model. Part I: Model description. *J. Phys. Oceanogr.*, **23**, 808–829.
- Redi, M. H., 1982: Oceanic isopycnal mixing by coordinate rotation. *J. Phys. Oceanogr.*, **12**, 1154–1158.
- UNESCO, 1981: The practical salinity scale 1978 and the international equation of state of sea-water 1980. UNESCO Tech. Papers in Marine Science No. 36, 25 pp. [Available from UNESCO Publishing Division, 1, rue Miollis, 75352 Paris, France.]
- Veronis, G., 1975: The role of models in tracer studies. *Numerical Models of Ocean Circulation*, National Academy of Science, 133–146.
- You, Y., and T. J. McDougall, 1990: Neutral surfaces and potential vorticity in the world's oceans. *J. Geophys. Res.*, **95**, 13235–13261.